LIMNOLOGY
and
OCEANOGRAPHY

ASLO

Limnol. Oceanogr. 9999, 2022, 1–16

doi: 10.1002/lno.12234

Coral reef erosion: In situ measurement on different dead coral substrates on a Caribbean reef

Ana Molina-Hernández,[1,2*] **Francisco Medellín-Maldonado**,[1,2] **Ines D. Lange**,[3] **Chris T. Perry**,[3] **Lorenzo Álvarez-Filip**[1]

[1]Biodiversity and Reef Conservation Laboratory, Unidad Académica de Sistemas Arrecifales, Instituto de Ciencias del Mar y Limnología, Universidad Nacional Autónoma de México, Puerto Morelos, Quintana Roo, México
[2]Posgrado en Ciencias del Mar y Limnología, Universidad Nacional Autónoma de México, Av. Ciudad Universitaria 3000, C. P. 04510, Coyoacán, Ciudad de México, México
[3]Geography, Faculty of Environment, Science and Economy, University of Exeter, Exeter, UK

Abstract

Widespread mortality of reef-building coral substantially reduces the capacity for reef growth and makes available extensive bare substrate areas that in the absence of coral recovery will be eroded by a variety of external and internal bioeroders. Here, we analyze rates of external erosion on six different types of carbonate substrates under in situ conditions over a 2-yr period. We measure vertical changes in the surface elevation of four species of recently dead corals afflicted by the stony coral tissue loss disease outbreak, and other two common types of calcareous substrates, long-dead *Acropora palmata* fronds and bare calcareous hardground, as a reference for "bare" carbonate substrates that occur widely in Caribbean reefs. The surface of the recently dead colonies experienced significant erosion after 2 yr of exposure, but at different rates depending on the species. Dead skeletons of *Orbicella faveolata* experienced the greatest rates of erosion after 2 yr at −9.9 mm (±3.2 mm); *Dendrogyra cylindrus* eroded −3.6 mm (±2.8 mm), *Pseudodiploria strigosa* −3.3 mm (±3.7 mm), and *Siderastrea siderea* −1.2 mm (±0.9 mm), while long-dead substrates remained unchanged. There was significant erosion in the presence of parrotfish grazing scars and of short algal turf mats, while crustose coralline algae cover and sand-and-high turf mats were not associated with significant changes in elevation, arguably indicating a protective effect. This study provides new insights into how and at what rates external carbonate erosion is shaping contemporary reefs at fine spatial and temporal scales.

Reefal ecosystems harbor a vast diversity of organisms, support complex trophic interactions, and provide critical goods and services to coastal human populations, including food, livelihoods, and protection from intense waves and storms (Woodhead et al. 2019). These functions are fundamentally controlled by the interactions between reef-building organisms and processes such as lithification, cementation, and dissolution, and by environmental factors that influence the construction of the carbonate reef framework (Perry and Alvarez-Filip 2018). In "healthy" reef systems, the general perception is that rates of coral carbonate production will exceed rates of erosion or framework losses, thus supporting the development and maintenance of complex reef structures (Glynn and Manzello 2015).

Indeed, the Holocene fossil record shows that high vertical accretion rates have characterized long periods of Caribbean reef development in many locations (but *see* Kuffner and Toth 2016; Toth et al. 2018), during which rates of carbonate production and accumulation exceeded rates of removal by breakdown, dissolution, bioerosion, and physical processes (Aronson et al. 2002; Perry et al. 2013, 2014; Hubbard and Dullo 2016). However, as contemporary coral assemblages shift away from historical states due to coral mortality and

---

*Correspondence: anamlhz@gmail.com

Additional Supporting Information may be found in the online version of this article.

Author Contribution Statement: A.M.-H. conceptualized and designed the study, performed fieldwork, analyzed the data, prepared figures and/or tables, write initial draft of the paper and approved the final draft. F.M-M. performed fieldwork, analyzed the data, prepared figures and/or tables, helped write and review drafts of the paper, and approved the final draft. I.D.L. performed fieldwork, analyzed the data, prepared figures and/or tables, helped write and review drafts of the paper, and approved the final draft. C.T.P. conceptualized and designed the study, helped write and review drafts of the paper, and approved the final draft. L.Á.-F. conceptualized and designed the study, performed fieldwork, helped write and review drafts of the paper, and approved the final draft.

disruption of ecological dynamics, the balance between carbonate production and erosional processes is being altered (Perry et al. 2014; Molina-Hernández et al. 2020). For example, in the Caribbean, mass mortality caused by coral diseases have significantly affected populations of reef-building coral species that were once widely dominant such as *Acropora* spp. and *Orbicella* spp. (Aronson and Precht 2001; Toth et al. 2019). This has resulted in ecological shifts in the composition of coral communities toward those defined by the dominance of nonframework building species (Perry et al. 2015; Cramer et al. 2021; Alvarez-Filip et al. 2022).

Such large-scale mortality events are concerning for reef ecosystems as they instantly reduce a reef's capacity to grow, whilst simultaneously facilitating substrate colonization by noncalcifying competitive organisms such as algae (Aronson and Precht 2001; Estrada-Saldívar et al. 2020), and various internal and external bioeroding organisms which can rapidly exploit dead coral substrates (Tribollet and Golubic 2011). Grazing sea urchins and parrotfishes are major drivers of erosion after coral mortality, and in the case of parrotfishes, this has been attributed to their exploitation of increased food resources in the form of epilithic and endolithic algae and cyanobacteria that colonize recently dead coral skeletons (Eakin 2001; Nicholson and Clements 2020; Taylor et al. 2020). Many species of parrotfishes use their beak-like jaws to bite and take up their food from the carbonate surface, eroding the reef substrate while feeding (Bellwood and Choat 1990). Likewise, newly dead coral skeletons are often rapidly infested by endolithic algae which, due to a higher light availability, increases its metabolic activity and biomass, driving enhanced rates of substrate chemical dissolution (Tribollet 2008; Pernice et al. 2020). Foraminifera and polychaetes may also colonize dead skeletons within the first months post-coral mortality, while boring sponges increase in abundance in dead substrates over the first 2–3 yr after tissue mortality, depending on environmental conditions (Kiene and Hutchings 1994; Tribollet and Golubic 2011; Schönberg et al. 2017). With the changes in coral assemblages and the resulting low-carbonate production rates that define many reefs, reef erosion is arguably becoming the dominant process in determining the fate and shape of contemporary perturbed reef ecosystems (Perry et al. 2018; Molina-Hernández et al. 2020).

Understanding the magnitude of these changes is thus important, but direct in situ measurements of erosion rates are not common (Bruggemann et al. 1996; Kuffner et al. 2019; Roff et al. 2019). Various measurements have been derived from the deployment of coral fragments (Grange et al. 2015), or by analyzing core samples from living or dead corals to derive the percentage of erosion/colonization by macroborers, but an accurate representation of the rate of erosion cannot be estimated with certainty using these methods as the time of exposure is unconstrained (Hernández-Ballesteros et al. 2013). The rates at which the bioeroding organisms wear down the substrate have also been estimated for various taxa (Glynn and Manzello 2015; Lange et al. 2020). For instance, by determining the $CaCO_3$ content in sea urchins' guts, the daily volume of $CaCO_3$ consumed by parrotfishes or the amount of material mechanically removed and dissolved by eroding sponges (Bruggemann et al. 1996; Conand et al. 1997; De Bakker et al. 2018). These studies have been useful for deriving indirect estimates of erosion rates at the site level, by integrating data from in situ census of the different internal and external bioeroders present at a specific reef site (i.e., abundance per area) with published species-specific rates of erosion of censored bioeroders (Perry et al. 2012; Lange et al. 2020). However, an important constraint with such estimations, is that they do not consider the potentially different resistance of distinct types of dead carbonate substrates (i.e., coral species) to erosion caused by variation in skeletal morphology, skeleton architecture, or skeletal density. For instance, erosion by encrusting sponges and other internal bioeroders has been shown to be positively correlated with coral skeletal density (Hernández-Ballesteros et al. 2013; Cosain-Díaz et al. 2021). This suggests that beyond the influence of the environment (e.g., temperature, pH, light availability), erosion in coral reefs likely also varies depending not only on the abundance of bioeroders, but also on the composition of benthic carbonate producers, and on the endolithic and epilithic communities that some bioeroding organisms target while feeding and which might itself be related to different substrate characteristics.

Here, we analyze rates of erosion under in situ conditions by measuring vertical changes in the surface elevation of recently dead corals over 2 yr. Four coral species (*Orbicella faveolata*, *Dendrogyra cylindrus*, *Pseudodiploria strigosa*, and *Siderastrea siderea*) were chosen for analysis following an outbreak of Stony coral tissue loss disease (SCTLD). This is an emergent coral disease that affects multiple coral species and has been identified as a significant driver of coral mortality and changes in reef functionality throughout the Caribbean (Alvarez-Filip et al. 2022). In the Mexican Caribbean, SCTLD left large numbers of dead corals and, consequently, new bare areas vulnerable for colonization and erosion in shallow reef areas (Estrada-Saldívar et al. 2021; Alvarez-Filip et al. 2022). This represented a unique opportunity to start an experiment where time of colony death could be constrained to a few days. In addition, we selected two other common calcareous substrates: long-dead *Acropora palmata* fronds and the bare calcareous hardground, as a reference for "bare" carbonate substrates that are widely abundant in the region of study.

Our main goals were to estimate rates of vertical erosion over a 2-yr period in different substrate types and, for recently dead substrates, to model the temporal trajectory of surface elevation change depending on the exposure time since coral soft tissue died. Furthermore, we explored if the vertical changes between intermittent survey intervals were related to ecological characteristics such as the occurrence of grazing scars, the type of benthic group colonizing the substrate surface, the identity of the carbonate substrate (i.e., species) and the time of exposure since death, and tested whether total erosion showed a relationship with species-specific skeletal density. These direct in situ measurements of erosion rates on different substrates (i.e., coral species) enable a better understanding of the spatial patterns of reef erosion, especially in areas with shifting community composition. Furthermore, determining the fate of dead coral skeletons may improve predictive models of changes in reef elevation with respect to the expected rise in sea level, and how reef erosion will regulate the dynamics of the coastline in future years.

Methods

Study site and disease outbreak context

In the Mexican Caribbean, SCTLD was first observed in the northern zone of Puerto Morelos region in June 2018. The disease caused a rapid and widespread die-off of over 20 coral species, killing entire colonies within a few weeks to several months, particularly at the onset of this outbreak (i.e., between the summer of 2018 and early 2019), which made available recently dead colonies for monitoring (Alvarez-Filip et al. 2022).

In September 2018, we selected a shallow reef site in Puerto Morelos called “La Catedral” (The Cathedral), named after a large patch of *D. cylindrus*, that rapidly died between September 2018 and February 2019 due to the SCTLD. This reef is situated in the back reef zone at a depth between 1.3 and 2 m and is part of a fringing reef system that runs parallel to the east coast of Quintana Roo from north to south, separated from the shoreline by a shallow lagoon. In general terms, this reef site is composed of patches of *A. palmata*, several of which are entirely or partially dead, patches of *O. faveolata*, scattered colonies of *P. strigosa*, *Siderastrea* spp., *Agaricia* spp., and *Porites* spp., and octocoral communities, a landscape commonly described for the back reefs of the region (Caballero-Aragón et al. 2020).

Carbonate substrates

We investigated erosion rates for six different type of carbonate substrates, four of them recently dead coral skeletons of *O. faveolata*, *D. cylindrus*, *P. strigosa*, and *S. siderea*. We selected these species because the following four criteria: (i) the species is a reef building coral afflicted by SCTLD, (ii) the species was previously present in relatively high numbers in the study area, (iii) the species has conspicuous colonies that are easy to identify and to tag, and (iv) the species has colonies with a known date of death (within 15 d). In addition, we selected two common, and long-dead bare carbonate substrates: dead but standing fronds of *A. palmata* and areas of bare calcareous hardground. Our rationale here was that these substrates are abundant in the region (Rodríguez-Martínez et al. 2014) and could provide information on later stages of erosion.

We selected at least six recently dead coral colonies from each of the four chosen species. All colonies were located with a minimum distance between colonies of at least 1 m, and in an area with a radius of 80 m. We selected coral colonies that were alive but showing visual signs of the disease in an active stage in January 2019 and that in due course died at a relatively similar time (i.e., between February and March 2019). It should be noted that coral colonies belonging to *D. cylindrus* are most likely ramets of the same large colony. This is because each “colony” was located within a patch of ca. 25 m^2, and this species is known to propagate via fragmentation following physical disturbances (i.e., asexual reproduction; Brainard et al. 2011). Therefore, estimations for this species may not reflect the variability that might be associated with nonclonal colonies. However, *D. cylindrus* is a rare species that exists in low abundance, and there were no other suitable colonies of this species within the study area. For the long-dead substrates, we followed a similar approach.

For *A. palmata* substrate, we chose one patch of dead standing and one of collapsed branches (40 m^2 area) showing signs of long-term exposure to the environment (e.g., smooth surfaces, branch-ends strongly flattened). Our measurements were made on colonies that were approximately ~2 m apart, still in growth position, but visibly shrunken in size, that we assume is due to the breaking and collapse of the larger and outer branches. The time of death of the *A. palmata* substrate is unknown, however considering the abovementioned characteristics compared to those observed in other patches of *A. palmata* for which the time of dead in the last 3–5 yr is known, the estimated period of death of the substrates we examined was likely at least 5–10 yr. For the bare calcareous hardground, which in the back-reef and crest zones of the northern part of the Mexican Caribbean has been previously characterized as Holocene reef framework (Ward and Brady 1979; Mulcahy 2014), we selected an area of ca. 30 m^2 of continuous flat shallow carbonate surface where we installed six reference markers.

In situ measurements of erosion

To measure vertical erosion rates of the selected carbonate substrates, we designed a method based on a three-component device: (1) a stainless-steel rod (8 mm in diameter) embedded with epoxy putty into a 15-cm deep hole drilled into the top of each colony skeleton; every rod thus serving as a fixed height reference post (Fig. 1a); (2) a removable device of our own design and manufacture that could be attached for measurements to the top of the rod, whose upper end has a welded hexagonal nut to ensure that the removable device was always secured following the same orientation. This device has two slotted compartments at each end (Fig. 1b), which serve to securely slot in and immobilize the third component; (3) a large caliper with a resolution of 0.02 mm (Fig. 1c). Once the caliper is inserted and immobilized, the caliper-depth-gauge (Fig. 1d) can be projected through a small

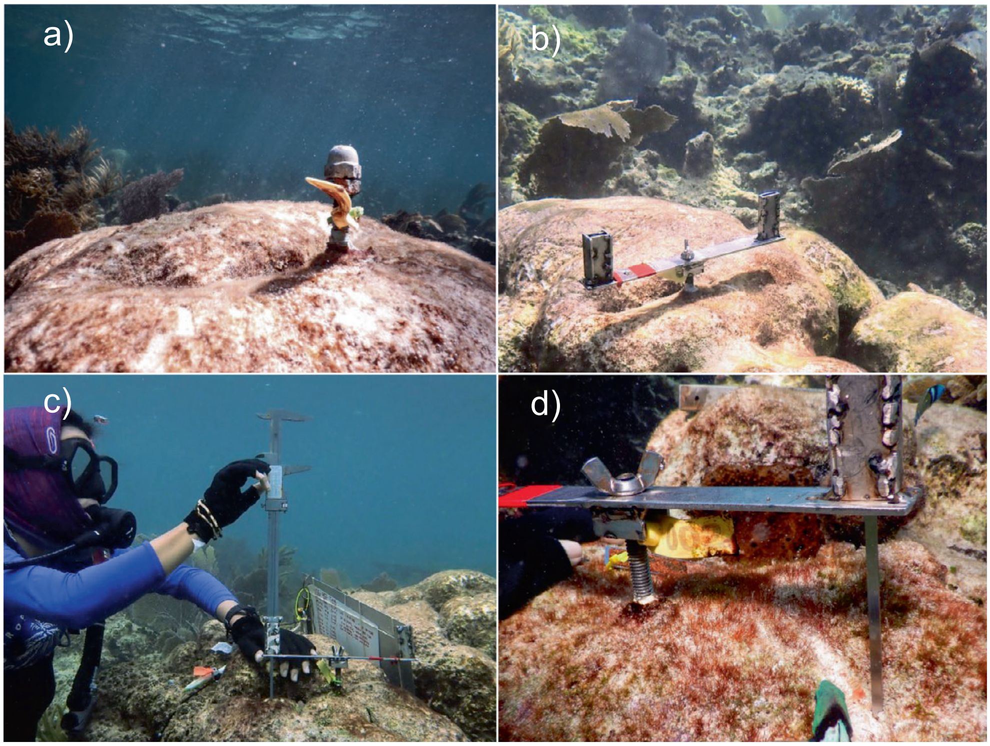

Fig. 1. Representation of the method for in situ measurements of erosion rates on carbonate substrates. (**a**) Stainless-steel rod embedded with epoxy clay on top of a *Orbicella faveolata* skeleton; (**b**) removable device with two compartments (one at each end), attached to a fixed rod, (**c**) caliper inserted (and immobilized) within the compartment in the removable stainless-steel device; (**d**) close-up on the extended caliper depth gauge making contact on the substrate surfaces.

hole located at the base of the slotted compartment. When the depth-gauge reaches the surface of the skeleton (i.e., making physical contact, Fig. 1d), the measurement was taken from the vernier scale. The system is designed so that the detachable device allows measurements at up to two fixed points in the vicinity of each rod, depending on the substrates' characteristics such as colony size and shape, but importantly at a distance between each measurement point and each rod of ca. 11 cm to minimize influence of the rod on substrate exploitation. In addition, we kept a photographic record of both the measurement shown by the vernier scale and of the surface where each measurement was taken. It should be noted that before taking measurements, we removed any loose sediment accumulated on the skeletons' surface by manually creating a current and, if necessary, using a small soft bristle brush to avoid damage to the substrate surface.

Initially, we set up the experiment to have a total of 12 measuring-points per species, however, by the end of the experiment we ended up with reduced numbers (Supporting Information Table S1). In three cases, this happened because the substrate' characteristics such as rugosity, size, and surrounding coral structures limited the insertion of the caliper in one of the compartments. In two other cases, the rod experienced movement on its axis (i.e., missing the precise point of measurement), and in one case, the overgrowth of a neighboring coral (*A. palmata*) impeded accommodating the caliper. The analyses of total vertical erosion only included measurement points fully tracked through all survey intervals. The first measurements were taken in February 2019, followed by four follow-up monitoring surveys to measure changes in the surface elevation of each substrate, with the last measurements taken in May 2021. Originally, measurements were planned to occur at 4-month intervals over a period of 2 yr, since Grange et al. (2015) reported changes in both biogenic dissolution and grazing around the 4th and 8th months of their experiment. However, due to COVID-19 pandemic mobility restrictions, the time between measurements was more variable (measurements approximately at 4, 8, 20, and 24 months after initial set-up, Supporting Information Table S1).

To determine if the erosion rates from point measurements are representative across the upper surface of dead coral colonies and to explore how variable erosion may be across the entire colony, we compared three-dimensional (3D) models of three of the monitored *O. faveolata* colonies and two of the monitored *P. strigosa* colonies over time. The colonies were photographed 2 yr apart, in January 2020 and March 2022 from all angles (75–82 photos per colony), with a foldable ruler placed in the proximity as a reference. The time period does not entirely match up with the actual survey interval and due to the low replication, this should only be seen as supporting and exploratory analysis. Photos were used to construct 3D models using the Structure-from-Motion software Agisoft Metashape Professional v 1.8.1 following the workflow described in Lange and Perry (2020). After scaling the models, dense point clouds were exported as .ply and aligned in the software CloudCompare v 2.10.2 through point pair picking and manual alignment using the fixed rods as reference points (Lange and Perry 2020). After isolating the dead coral colonies from the surrounding reef by drawing a polygon around them, the distance between point clouds was then computed for (1) the top of the colony and (2) the entire surface of the dead coral colonies using the "M3C2 Distance" plugin. This algorithm computes signed and robust distances between two clouds along the normal surface direction instead of using closest points, the latter of which may underestimate small distances (Lague et al. 2013; James et al. 2017). The average erosion rate was determined from the histogram of absolute distances projected onto the 2022 cloud, taking into account only points that lost distance as opposed to gaining it (mainly the case at the sides of colonies and indicating the growth of turf algae mats). To improve accuracy of estimates, we also removed points with projected uncertainties of ≥0.0013 and points with a distance of ≥5 cm (indicating faulty projections or removal through forces other than biological erosion). The average distance between point clouds was divided by the number of days between survey dates and multiplied by 365 to yield annual vertical erosion rates (comparable to direct measurements).

Benthic colonizers and parrotfish feeding scars

Along with measurements taken at every survey interval, we recorded the benthic group that colonized the surface of each carbonate substrate. This was done at the exact same point where each measurement was taken (i.e., where the calipers' depth-gauge has contact with the surface, Fig. 1d). On recently dead coral substrates, observed groups included short turf algal mats (turf); short turf-and-sand mats (TAS), sand-and-high turf mats (STA), and crustose coralline algae (CCA) (Supporting Information Table S2); while on the long-dead bare substrates, we additionally observed sand, a boring sponge (in only one of the substrates at the last survey interval), and fleshy macroalgae (on three occasions). We registered this information to explore if there was an association between the benthic group colonizing recently dead coral substrates and the changes in the surface elevation that were measured over the four consecutive survey intervals, following the assumption that different benthic groups could indicate different underlying processes in terms of erosion/accretion. For instance, the occurrence of CCA adds a carbonate layer that can protect dead reef substrate against bioerosion and facilitates the recruitment of coral larvae (Barott and Rohwer 2012). In contrast, the occurrence of short turf and TAS likely indicates that algae thali on the surface is being constantly grazed, and therefore that the surface is potentially more often eroded, as herbivores including parrotfish and sea urchins scrape the reef surface while feeding (Bellwood and Choat 1990).

We also recorded the absence/presence of feeding scars on planar photographs of surveyed surfaces. Although we were able to observe up to three different types of feeding/eroding scars (i.e., parrotfish bites, sea urchins' bites, and encrusting sponge oscula; Supporting Information Fig. S1), only the parrotfish scars were used in the analysis due to their conspicuousness and consistency, which facilitated their identification from photographic records. Other scar types were observed only sporadically. The presence of parrotfish scars was registered at group level when a minimum of five marks/scars was present on the top of the colony surface surrounding the measurement points. We assumed that the substrates with feeding scars would experience a greater change in surface elevation, since bites on the surface directly wear down the carbonate substrate (Bruggemann et al. 1994*a*).

Skeletal density

In order to explore if there was a relationship between skeletal density (g $CaCO_3$ cm $^{-3}$), and total erosion we obtained 4–10 cores (depending on the species; Supporting Information Table S1) for *O. faveolata*, *D. cylindrus*, *P. strigosa*, and *S. siderea* colonies. Because the process to extract the samples (i.e., drilling the surface) could compromise the structure of the substrates that we were planning to observe, cores were obtained from neighboring colonies located no more than 10 m distance from those that we tagged and measured during the experiment, and that died in the same time interval (within a few days) in early 2019. It is important to mention that *D. cylindrus* samples actually correspond to the same patch where we worked during this experiment, since coral samples from that patch were collected in 2015 for a separate study (Cruz-Ortega et al. 2020). The *D. cylindrus* samples were 10 cm in diameter and 10–20 cm in length. While samples from *O. faveolata, P. strigosa*, and *S. siderea* were 3 cm in diameter and 5–15 cm in length.

Extracted skeleton samples were cut perpendicular to their growth axis into ~9-mm-thick slabs which were washed and dried in an oven at 60°C for 48 h (Carricart-Ganivet and Barnes 2007). Dry slabs were X-radiographed and digitalized. During the scan, the slabs were accompanied by an aragonite standard consisting of a wedge of known thickness and density (2.83 g $CaCO_3$ cm^{-3}). Resultant digital images were corrected to avoid density alterations produced by the "heel effect" and the "square law" and analyzed using the ImageJ software (v. 1.8.0). Skeletal density was measured along each slab following the axis of maximum growth to where alternating density bands were identifiable, following the method described by Carricart-Ganivet and Barnes (2007). Densities are reported in Supporting Information Table S1.

Bioerosion estimates from reef surveys

In June 2019, after the onset of the SCTLD and approximately 3 months after the corals tracked in this study had died, we estimated the reef carbonate budget at la Catedral reef using the census-based *ReefBudget* approach (Perry and Lange 2019). In addition to estimating carbonate production, this method estimates the rate of bioerosion at a reef scale, and can be used to identify the primary biological drivers of reef accretion/erosion. The total bioerosion rate is obtained from the abundance of bioeroders (i.e., in situ census) and species-specific rates of carbonate erosion (extracted from literature) for parrotfishes (10 species), sea-urchins (3 species), boring sponges (8 species), and microbioeroders (average rate). For parrotfish, abundance and size of each fish was measured across eight belt-transects (30 m length × 2 m width), whereas sea urchins and boring sponges were counted in six belt-transects (10 m length × 1 m width). Microbioerosion rates were estimated from average published rates multiplied by available substrate (from benthic surveys along six 10 m transects). The total erosion rate is reported in kg $CaCO_3$ m^{-2} yr^{-1}.

Data analyses

We calculated and plotted the total vertical erosion observed after 2 yr of exposure for recently dead coral colonies and the long-dead bare carbonate substrates (Fig. 2). This facilitated a first broad comparison of the erosion rates between the different substrates (Fig. 2). As we observed substrate-specific differences in total erosion, a generalized linear mixed model (GLMM) was fitted to explore the relationship between total erosion in recently dead coral substrates and skeletal density at species level. Unlike other regression models, GLMM allows for the inclusion of random effects to control aspects of experimental design (Schielzeth and Forstmeier 2009). In this analysis, total change in surface elevation (millimeters) was specified as a response variable (i.e., final measurement minus initial measurement of each data point) and the average skeletal density of the species as predictor. Here, colony identity was included as a random effect to control for variation associated with the nature of our study design (paired measurements per colony).

Although the total average change in surface elevation was negative in all types of substrates throughout the experiment, we observed both negative (i.e., erosion) and positive (i.e., accretion) changes at distinct survey occasions and measuring points. Therefore, we explored the relationship between the change in surface elevation (mm) observed over each time interval (i.e., interval 1 = 2^{nd} measurement − 1^{st} measurement, interval 2 = 3^{rd} measurement − 2^{nd} measurement, interval 3 = 4^{th} measurement − 3^{rd} measurement, interval 4 = 5^{th} measurement − 4^{th} measurement) and the different covariates tracked at the end of each time interval by means of a GLMM, for which we specified the change in elevation (i.e., millimeters) measured at each interval as the response variable, and as predictors (i.e., fixed factors) we specified the presence/absence of parrotfish bite scars, the benthic group colonizing the substrate (i.e., short turf mats; TAS; STA, CCA), and the time elapsed since

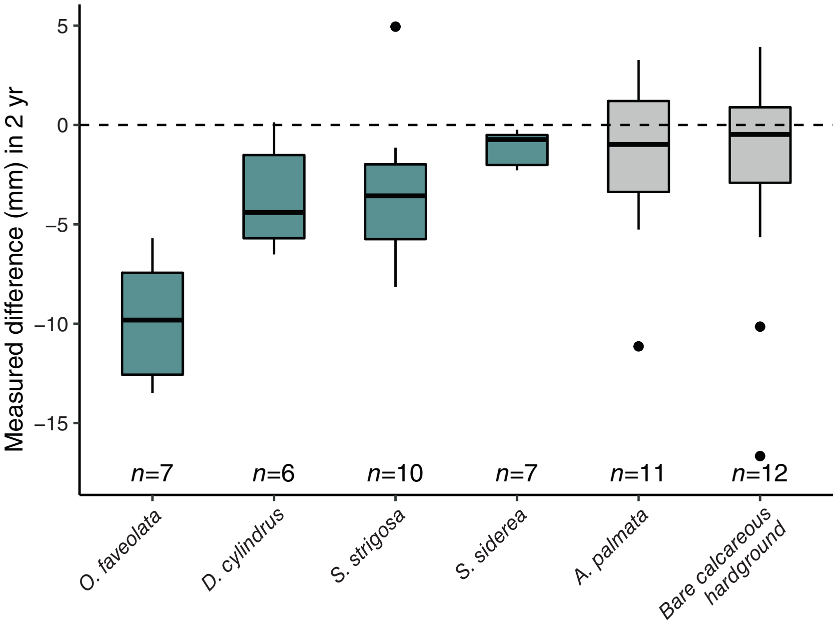

Fig. 2. Total change in carbonate substrate elevation (mm) after 2 yr of exposure. (**a**) Green boxes are for species whose mortality occurred a couple of days before the beginning of the experiment. Gray boxes are for long-dead substrates, whose surface has been exposed for several years longer. Sample size per species is reported at the bottom of the graph.

mortality (in months). Species, colony identity, and the measuring point were treated as random factors within the model expression to account for design and repeated measurements. The long-dead bare carbonate substrates (*A. palmata* and the hardground) were not included in this analysis (as time of dead was unknown; *see* "Methods" section).

To explore the trajectory of elevation change of the substrates over time, we fitted a GLMM where we specified an interaction between the fixed continuous factor "time" (i.e., accumulated months of exposure after coral tissue died) and the categorical fixed factor "coral species" (i.e., four species: *O. faveolata*, *D. cylindrus*, *P. strigosa*, and *S. siderea*) as predictors of surface elevation change (i.e., millimeters). For this analysis we included only recently dead substrates so that we could control the exposure time after coral tissue mortality. We again specified colony identity as a random factor, as well as random effects for individual measuring points to account for the repeated measures over time (i.e., a trend analysis), and we specified random slopes for the continuous variable of time (Schielzeth and Forstmeier 2009). We compare the modeled trajectories of the four species over time based on standardized model coefficients and their 95% confidence intervals (CI). First, we compared coefficients (± 95% CIs) obtained for the four species at the four measurement times (i.e., at 4th, 8th, 20th, and 24th months of exposure) against zero to identify the time at which a significant change in surface elevation (i.e., erosion) occurred. Second, we compared the coefficients (± 95% CIs) obtained for the four species against each other for each point in time. Overlapping CIs indicate similar rates of change in surface elevation, whereas CIs not overlapping indicate different erosion rates among species. All mixed-effects models were fitted using the R function *lmer* from the package "lme4." Model assumptions were validated using residual plots.

Finally, model coefficients from the surface elevation analysis were used to predict how long it would take for typical colonies of *O. faveolata*, *P. strigosa*, and *D. cylindrus* in the Mexican Caribbean (the three species that were eroded significantly during our study) to erode from the surface to the bottom, assuming that rates of erosion remained constant over time and only occurred from the top. For this prediction, we used the average height reported for *O. faveolata* (mean height = 34.45 cm; ± 24.99), *D. cylindrus* (mean height = 38.95 cm; no SD reported), and *P. strigosa* (mean height = 24.76 cm ± 17.08) in the Mexican Caribbean (González-Barrios and Álvarez-Filip 2018). With our rates of vertical erosion and the skeletal density, we also estimated how much mass of calcium carbonate could be removed per square meter substrate per year (kg $CaCO_3$ m^{-2} yr^{-1}, units referred to as G) for each studied species assuming a planar surface. For this, we followed the same rationale used to estimate calcification rates for coral species, where calcification rate (g $CaCO_3$ cm^{-2} yr^{-1}) = density (g cm^{-3}) × linear growth rate (cm yr^{-1}). In our case, planar erosion rate (g $CaCO_3$ cm^{-2} yr^{-1}) = density (g cm^{-3}) × vertical erosion rate (cm yr^{-1}).

Results

In situ measurements of vertical erosion on recently dead coral skeletons indicated that after 2 yr of exposure, the average change in reef surface elevation was negative (-4.4 ± 4.2 mm SD). At the species level, the total vertical changes that we observed over the 2 yr, correspond to annual rates of erosion of -4.9 ± 1.6 mm yr^{-1} in *O. faveolata*; in *D. cylindrus* -1.8 ± 1.4 mm yr^{-1}; in *P. strigosa* -1.7 ± 1.9 mm yr^{-1}; and in *S. siderea* -0.6 ± 0.4 mm yr^{-1} (Fig. 2). In contrast, the two long-dead bare substrates presented standardized annual rates of -0.9 ± 2.0 mm yr^{-1} in *A. palmata* fragments; and -1.2 ± 3.0 mm yr^{-1} in the bare calcareous hardground (note the large standard deviation associated with these long-dead substrates). We found that erosion on recently dead substrates correlated negatively with skeletal density, with vertical change highest in the low-density *O. faveolata* ($p < 0.01$; marginal $r^2 = 0.31$; Supporting Information Fig. S2). The comparison of 3D models of a subset of recently dead coral skeletons (comparing colonies in 2020 and 2022) yielded very similar vertical erosion rates across the top surface of coral colonies (-4.8 ± 0.7 mm yr^{-1} for *O. faveolata* [$n = 3$] and -1.5 ± 0.4 mm yr^{-1} for *P. strigosa* [$n = 2$]). The models also show that erosion took place mostly at the top surface, whereas the lower sides of colonies were stagnant or even gaining volume due to overgrowth by turf algal mats (Fig. 3).

The surface of the measuring points was most often covered (i.e., in 94% of the surveyed occasions) by algal mats (i.e., short turf, short turf-and-sand, or STA), while CCA was observed in only 6% of the occasions throughout the 2-yr experiment. In contrast, long-dead bare substrates were overgrown by turf algal mats in just one-third (37%) of the occasions, whereas CCA and sand occurred at 59% of the measuring points throughout the study period, along with two other types of coverages that were not observed in recently dead substrates, namely encrusting sponges and fleshy macroalgae in around 5% of the occasions (Supporting Information Table S2). Another difference we observed between recently dead substrates and long-dead bare substrates was the direction of elevation change that we measured by the end of the experiment. After 2 yr of exposure, we registered a very low proportion of positive values (i.e., accretion) in the recently dead coral skeletons: *O. faveolata* and *S. siderastrea* presented 0% positive values; and *D. cylindrus* and *P. strigosa* presented 10% and 16%, respectively. In contrast, the long-dead substrates *A. palmata* and bare calcareous hardground showed positive accretion in 36% and 33% of replicates, respectively.

We found that negative change in surface elevation measured over each consecutive monitoring interval (i.e., erosion) was significantly higher in the presence of parrotfish bite

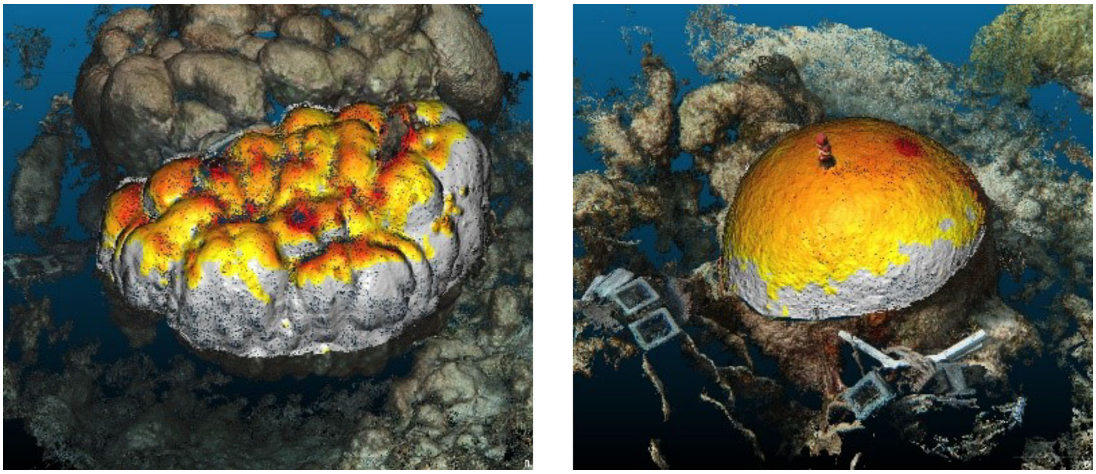

Fig. 3. Examples of 3D model comparison for colonies of *Orbicella faveolata* and *Pseudodiploria strigosa*, showing highest erosion rates at the top surface of colonies. Color scale depicts small changes in yellow (0–3 mm) and large changes in red (>10 mm), gray areas indicate no change or positive changes on colony surface comparing 2020 and 2022 models.

scars, and of different benthic colonizers, the TAS, and short turf mats (Fig. 4; Supporting Information Tables S3, S4). The other groups showed no positive or negative effect on average vertical change, visible by CIs overlapping with the 0 line in Fig. 4. The GLMM analysis also showed that the rate of erosion was constant over time, since there were no significant differences in elevation change among consecutive survey intervals, indicating a linear trend in the surface elevation of recently dead substrates (Supporting Information Table S4).

Associated census-based *ReefBudget* surveys performed following the onset the study at La Catedral reef also indicated that the main bioeroders in this reef are parrotfish (particularly *Sparisoma viride*) which were estimated to contribute 70% of total erosion (1.20 kg $CaCO_3$ m^{-2} yr^{-1} ± 1.67), while encrusting sponges contributed 15% (0.26 kg $CaCO_3$ m^{-2} yr^{-1} ± 0.23), sea urchins (mainly *Diadema antillarum)* contributed 1% (0.01 kg CaCO3 m^{-2} yr^{-1} ± 0.01) and microbioerosion, which was estimated based on available carbonate substrate (Perry and Lange 2019) contributed 14% (0.25 kg $CaCO_3$ m^{-2} yr^{-1} ± 0.25). Overall, we estimate bioerosion pressure at La Catedral reef to be 1.73 kg $CaCO_3$ m^{-2} yr^{-1}. Consistent with the census of bioeroders, we observed three different types of bioeroding scars on the surfaces of selected substrates from pictures taken during monitoring, scrapes caused by parrotfish, oscula from the encrusting sponge *Cliona delitrix*, and scars from sea urchins (Supporting Information Fig. S1). Based on the ReefBudget surveys at La Catedral reef, we also estimated the average rate of carbonate production at 2.5 kg $CaCO_3$ m^{-2} yr^{-1} (±2.0 kg $CaCO_3$ m^{-2} yr^{-1} SD). This results in a low yet positive net

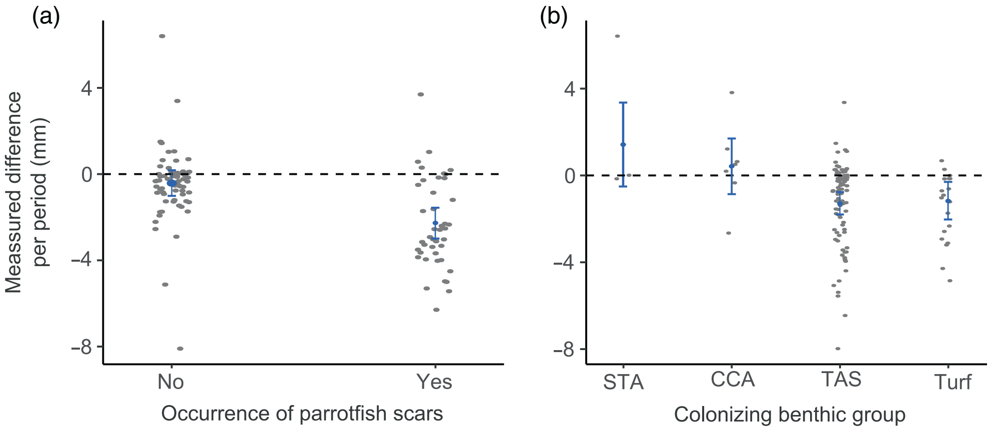

Fig. 4. Predictors of the surface elevation change (millimeters) measured over each consecutive monitoring interval. (**a**) Occurrence of parrotfish scars; (**b**) type of colonizing benthic group (STA, CCA, TAS, and turf). Dots represent all measurement taken through the 2 yr of exposure at each of the four consecutive intervals. Error bars represent the 95% CIs of the linear mixed-effect models. 95% CIs that do not overlap with the zero line represent a significant result.

carbonate production rate at this site equal to 0.8 kg $CaCO_3$ m^{-2} yr^{-1}. Notably, during the post-outbreak censuses, no living colonies of *P. strigosa*, *D. cylindrus*, and *S. siderea* (species afflicted by the SCTLD) were recorded within the survey transects. However, we did observe several recently dead skeletons of *P. strigosa* and *S. siderea*.

The analysis of the trajectory of vertical erosion over time (Supporting Information Table S5) showed a significant interaction between time and coral species ($p < 0.01$, Supporting Information Table S6), which indicates that the effect of exposure time on the surface elevation depends on the identity of the substrate (i.e., coral species) and, similarly, the effect by species depends on the exposure time since soft coral tissue died. Overlapping CIs of trajectories indicate similar rates of erosion across all species after 4 months exposure, but increasingly higher erosion in *O. faveolata* as time progressed (Supporting Information Table S7). This resulted in a significantly greater loss after 24 months of exposure in comparison to the rest of the species that lost their tissue at the same time (Fig. 5). Erosion rates of other species remained similar (respective 95% CIs overlapping each other throughout the entire study period), and all but *S. siderea* showed significant erosion by the end of the study period (CIs not overlapping with 0). However, as all replicates of *S. siderea* showed a negative vertical change after 24 months of exposure (Fig. 2), this suggests that the overlap of CI with 0 in the temporal trend analysis resulted from some positive accretion in intermediate time intervals and the overall very small change since initial measurements.

When translating rates of vertical erosion derived from the temporal trend analysis to planar rates of erosion (i.e., the mass of calcium carbonate being removed per square meter per year if that colony covered the entire surface area) using species-specific skeletal densities, we find that *O. faveolata* loses 5.6 kg of $CaCO_3$ m^{-2} yr^{-1} (95% CI = −7.1 G to −4.1 G); *D. cylindrus* lost 3.4 kg of $CaCO_3$ m^{-2} yr^{-1} (95% CI = −5.7 G to −1.0 G), and *P. strigosa* loses 5.0 kg of $CaCO_3$ m^{-2} yr^{-1} (95% CI = −7.2 G to −2.9 G). Furthermore, under a scenario with the same environmental conditions and fixed rates of erosion over time, the analysis of the vertical erosion rates suggests that an average-sized dead colony of *O. faveolata* (34.45 cm ± 24.99 mean height) would be completely eroded by biological erosion processes within ~80 yr; a *D. cylindrus* colony (mean height = 38.95 cm; no SD reported) would be fully eroded within ~240 yr; and a *P. strigosa* colony (mean height = 24.76 cm ± 17.08) would disappear within ~340 yr.

Discussion

Although the impacts of mass mortality events in terms of coral cover and diversity have received much attention, less attention has been given to the actual fate of skeletons left standing after coral death. Here, we show that the surface of colonies that experienced total mortality due to SCTLD, exhibited a considerable loss in vertical elevation after 2 yr of exposure. Our results also show that dead carbonate structures eroded at different speeds depending on the identity of coral species. Dead skeletons of *O. faveolata* experienced the greatest

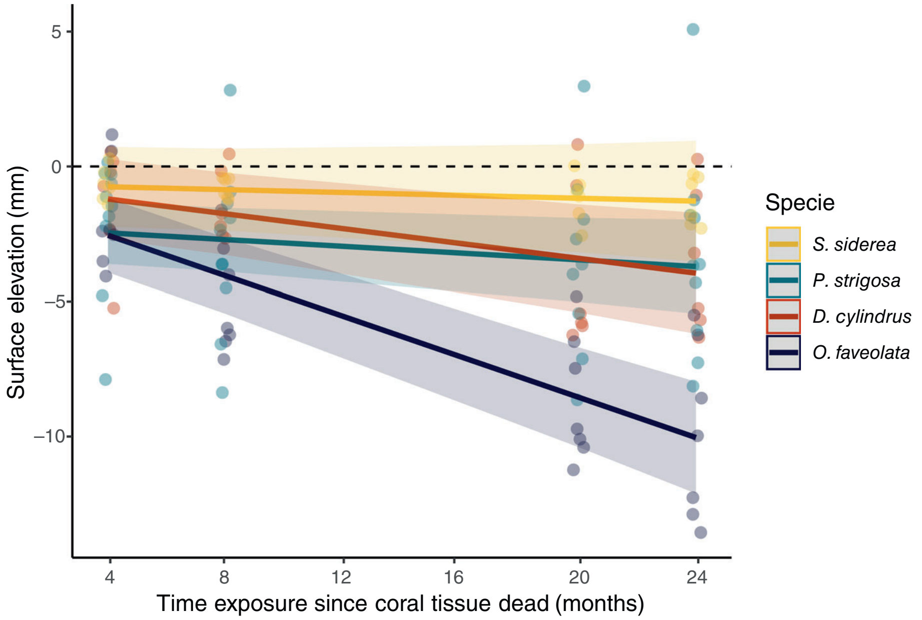

Fig. 5. Fitted regression lines and 95% CIs derived from the linear mixed effect model for each species: *Orbicella faveolata* in purple, *Dendrogyra cylindrus* in red, *Pseudodiploria strigosa* in blue, and *Siderastrea siderea* in yellow. Horizontal dashed line denotes the reference of initial surface elevation.

loss in surface elevation, whereas the surface of dead *S. siderea* colonies experienced minimal erosion over 2 yr of observations. Interestingly, when we analyzed the estimated changes in elevation by interval, we found that external factors such as the presence of parrotfish grazing scars and the presence of short algal turf mats were associated with negative changes in surface elevation; while substrates with high CCA cover and STA mats had no significant change in elevation, arguably indicating a protective effect (Chisholm 2003; Adam et al. 2018; Tebbett et al. 2020). This study provides new insights into how and at what rates external carbonate erosion is shaping contemporary reefs at fine spatial (i.e., at species level) and temporal scales (4 months to 2 yr). Our findings are particularly relevant in the context of recently increasing mass coral mortality events and identifies substrates with higher vulnerability to erosion and the potential implications for the integrity of the coral reef's structure. These data also give an indication of the pace at which some bare reefal areas are currently eroding.

Average vertical erosion ranged from nearly half a cm vertical loss per year in *O. faveolata* to no change in the long-dead standing *A. palmata* skeletons and the bare calcareous hardground substrates. Few other studies have managed to directly measure rates of vertical erosion in carbonate structures, although we note that rates of erosion for *O. faveolata* are consistent with long-term estimates reported by Kuffner et al. (2019) for the same species (-5.5 mm yr^{-1} ± 3.2 SD) on a shallow patch reef in Florida. The rates are remarkably close considering the difference in exposure time (2 yr vs. 17 yr), and potential uncertainties associated with the use of different methods (e.g., devices) to measure substrate elevation here and in Florida (which interestingly, although independently designed, follow a similar approach, *see* description in Kuffner et al. (2019)). Comparable characteristics between studies include a shallow environment, the intensity of bioerosion based on the *ReefBudget* methodology (-1.7 kg $CaCO_3$ m^{-2} yr^{-1} in this study vs. -1.9 kg $CaCO_3$ m^{-2} yr^{-1} in Florida), and a low skeletal density of the reef framework (1.1 g $CaCO_3$ cm^{-3} in this study vs. 1.3 g $CaCO_3$ cm^{-3} in Florida; Manzello et al. 2018), which could explain the close agreement between rates. In another study in Florida, Hudson (1977) determined an average vertical erosion rate of -6.7 mm per year for the sister species *Orbicella annularis*, based on the measurement of superficial missing parts of the skeleton observed on coral slab x-radiographs that corresponded to the corals' growth period between 1970 and 1974. In contrast, two other studies estimated much lower vertical erosion for *O. annularis* over two periods following a bleaching event in Long Cay, Belize (Roff et al. 2015, 2019). Based on the species extension rate and the percentage of area bored by internal eroders on the ramets, the authors calculated an average vertical loss of -0.7 mm yr^{-1} for the period between 1998 and 2011; and -1.1 mm yr^{-1} between 1998 and 2018. Differences to the data from Florida could be attributed to the high density of the *O. annularis* skeletons sampled in Belize (1.9 g cm^{-3}), although it is likely that methodological limitations (e.g., no permanent markers were used in Belize) also need to be considered when comparing erosion rates between the studies conducted in Belize and the reports from Florida and this study. Measurements taken at fine temporal scale can detect different patterns of erosion (or even accretion) over time, which may be otherwise masked (Viles and Trudgill 1984).

Total change in the surface elevation of long-dead standing *A. palmata* skeletons and the bare calcareous hardground were not significant after 2 yr, owing to the larger spread of data and the occurrence of positive changes in elevation (i.e., accretion, *see* Fig. 2). This was different from recently dead substrates and might not only be related to the intrinsic characteristics associated with the species (e.g., skeletal microstructure, density, porosity, morphology), but also with development and maturation of eroding and non-eroding communities over time (Hutchings 1986), or to the presence of internal inorganic cementation which further increases density of dead substrate. Our measurements of changes in *A. palmata* surface elevation were made on a basal, consolidated part of standing fronds. Observed current rates of erosion therefore may not necessarily correspond to what recently dead skeletons of the same species may exhibit, including accelerated rates of erosion. For instance, it has been reported that due to its branching morphology, after mortality events, the external branches of *A. palmata* colonies are more vulnerable to wave-breaking and rubble displacement, followed by intensive erosion of detached fragments (Sano et al. 1987; Sheppard et al. 2002). Despite the potential changes in structural complexity and elevation that the *A. palmata* stands could had experienced in the past, the absence of accelerated erosion in contemporary flattened stands is relevant for understanding the geoecological functions that even degraded habitats can provide (Morillo-Velarde et al. 2018; Perry and Alvarez-Filip 2018).

The bare calcareous hardground did not present net erosion either, but a relative stasis in its overall elevation. Both types of long-dead bare substrates are dominant in the back reef and crest in coral reefs within this region, so their relatively stable elevation and apparent resilience to biological erosion provide some hope that such substrates will not experience rapid erosion. This is interesting given the low budgetary state that many reefs in this region, including La Catedral, are experiencing and the evidence of vertical flattening occurring in other reefs in the Caribbean and the Atlantic (e.g., reefs in all four sites studied by Yates et al. (2017) within the region showed elevation and volume losses) that threatens their integrity and functionality (Alvarez-Filip et al. 2009; Yates et al. 2017; Perry et al. 2018; Toth et al. 2019).

Our models show that significant changes in surface elevation occurred where parrotfish bite scars were present. These fish, particularly excavating species (i.e., *S. viride*, *Scarus guacamaia*, *Scarus coelestinus*; Adam et al. 2018) use their powerful beak-like jaws to scrape the carbonate structure (Bruggemann et al. 1994*a*, 1996) in order to access the high-protein community of epilithic and endolithic microorganisms which inhabit the upper layer of dead coral skeletons (ca. 1–40 mm depth, Tribollet 2008), often, leaving grazing scars that mark the location were carbonate mass was removed. Parrotfish have been identified as the major force of erosion in many tropical reefs in the Caribbean, particularly after the demise of the sea urchin *D. antillarum*, which prior to the 1983 mass mortality event had been reported to exert significant herbivory and erosion pressure where abundant (Perry et al. 2014; Lessios 2016). Consistent with this, our census data confirmed that parrotfish, and specifically *S. viride*, are by far the dominant agents of external bioerosion at La Catedral reef.

Likewise, significant negative changes in surface elevation were observed where short turf mats and short turf-and-sand mats were present. Although algal turfs present an anchoring system that might exert some microstructure damage as roots attach to the coral skeleton (Trenhaile 2011; Phillips et al. 2019), this benthic group is not considered to be an active erosive agent. Yet, its presence has been related to the feeding preferences of herbivores and detritivores including major eroders such as parrotfish. In this regard, we observed a higher proportion of parrotfish bite scars on colonies with presence of TAS and turf mats (Supporting Information Fig. S4). In addition, the constant feeding pressure of those eroding species can maintain short turf algae mats over time while limiting the overgrowth of other benthic organisms including thick taller algae turf mats or large macroalgae (Diaz-Pulido and McCook 2002; Adam et al. 2015). Species like *S. viride* and *Scarus vetula*, have been found to mainly target short turfs while searching for epilithic and endolithic prey, with preference for convex and flat upper surfaces, boulder habitats, and species like *O. faveolata* (Bruggemann et al. 1994*a*; Adam et al. 2015, 2018). In this sense, pressure exerted by parrotfishes likely drove the observed linear trends in the reef surface elevation, but different trends might derive specifically from micro and macro internal erosion (Tribollet and Golubic 2011; Grange et al. 2015).

On the other hand, CCA, and the sand-and-large turf mats had no significant effects in our model. CCA has been reported to yield significant accretion in tropical habitats under certain environmental conditions, suggesting their presence may limit the colonization of erosive capabilities of external bioeroders thanks to the addition of thin layers of calcium carbonate on the bare surfaces (Chisholm 2003). Mats loaded with sand and fine sediment could also inhibit erosion by limiting colonization by internal bioeroders such as endolithic algae, and keeping grazing-bioeroding organisms away, as that coverage is targeted to a lesser extent by these organisms (Hutchings et al. 2005; Adam et al. 2018; Tebbett et al. 2020).

Differences among substrates in total erosion were related to the species identity, which is a proxy for certain traits that vary among species, such as porosity, shape, and skeletal density, all of which have been shown to influence rates of erosion (Bruggemann et al. 1994*a*,*b*; Adam et al. 2018). We found that substrates with lower skeletal density experienced greater vertical erosion rates. Low-density coral skeletons are characterized by reduced compressive-and-tensile strength and stiffness, characteristics that increase the possibility of skeleton breakage and fracture (Chamberlain 1978; Hughes 1987). Mechanical characteristics related to low skeletal density may also explain why grazers like parrotfish target low-density corals, as this characteristic seems to facilitate deeper bites and therefore higher energy return per bite (Bruggemann et al. 1994*a*,*b*). Bruggemann et al. (1994*a*) reported faster rates of erosion by parrotfish on low-density substrates including *Colpophyllia natans*, *Diploria* spp. (as listed by the author prior to the split into two genera: *Diploria* and *Pseudodiploria*), *O. annularis*, and *Madracis miriabilis*, while high-density skeletons such as *Acropora* spp., and *Agaricia* spp., eroded slower. Although we did not include the long dead *A. palmata* in the analysis (as time of death was unknown; *see* "Methods" section), our results for that substrate align with the relationship we describe, since this species has a high skeletal density (Table S1) and experienced no significant erosion at our study site. Interestingly, when it comes to internal macrobioerosion (which we did not focus on) and skeletal density, an opposite relationship has been reported to occur i.e., higher internal bioerosion occurring as skeletal density increases. This is probably because internal macroeroders such as polychaetes, bivalves, and so on, seek shelter, and therefore may favor denser, more resistant skeletons (Hernández-Ballesteros et al. 2013; Cosain-Díaz et al. 2021).

The loss of the surface elevation (i.e., vertical erosion) that we observed on the recently dead substrates, was the result of a gradual cumulative effect over 2 yr of exposure with rates varying depending on substrate identity (i.e., species). *O. faveolata*, experienced greater loss of elevation after only 1 yr, than *D. cylindrus* and *P. strigosa* over the full exposure period, while the surface elevation of *S. siderea* remained relatively stable over the 2 yr of exposure. The rather constant erosion rates observed in the substrates indicate that the pressure exerted by the bioeroders has been sustained over time, at least during the 2 yr of observation. Consistent with such patterns, the bioeroding activity of parrotfishes has been reported to intensify after coral mortality, likely, influenced by the settlement and maturation of euendolithic communities that are targeted by external grazer but which also enhance rates of internal dissolution in coral skeletons (Grange et al. 2015; Pernice et al. 2020). Post-mortality-enhanced rates of erosion can persist for several months to years, particularly in shallow reefs (Chazottes et al. 1995; Grange et al. 2015; Russ et al. 2015).

It is, however, possible that rates of erosion could speed up or slowdown in the future (i.e., beyond the 2 yr that our experiment lasted) as further disturbances occur in the ecosystem, or as new assemblages of benthic organisms establish. For instance, encrusting sponges tend to colonize dead skeletons 2–3 yr after coral mortality (Kiene and Hutchings 1994), potentially increasing erosion rates in the near future. Conversely, colonization by calcifying organisms such as CCA and coral recruits could restrict erosion, and favor reef accretion. In the longer term, dissolution of coral skeletons by boring sponges and endolithic algae could also intensify with predicted increases in carbon dioxide in the oceans, and increased colony breakage under high-energy events potentially causing abrupt erosion events (Enochs et al. 2015). Our modeled trajectories of erosion indicate nontheless, that despite the differences in the rate of erosion between species (e.g., *O. faveolata* eroding faster than *D. cylindrus*), under a scenario where our estimated rates were to remain stable, colonies that died due to SCTLD could disappear over the next decades to centuries, depending on the species and their size. From the human perspective such time frames span several generations, but contemporary management actions are needed to counteract the effect of the mass mortality caused by the SCTLD (Alvarez-Filip et al. 2022) and to preserve the provisioning of the physical and ecological functions that not only living reef framework but also dead skeletons still provide even without the living calcifying tissue (Rogers et al. 1982; Morillo-Velarde et al. 2018).

The bioerosion rates based on a census approach, such as the one proposed within the *ReefBudget* methodology, describe how much consolidated-carbonate a reef site loses per area over time, but do not describe how that erosion is actually spatially distributed (Perry and Lange 2019; Lange et al. 2020). Integrating species-specific rates of vertical erosion as those reported here, together with species-specific density values, could yield more accurate estimates of the amount of calcium carbonate removed per reef area (a rate known as “planar erosion rate,” with units commonly expressed as kg $CaCO_3$ m^{-2} yr^{-1}). This approach could also help in reconciling to what extent reef-scale erosion that is currently estimated from bioeroder abundances is in fact altering the reef framework. An example of such an approach is presented in Kuffner et al. (2019), where the authors used their estimated vertical rate of erosion of *O. faveolata* to determine the planar erosion rate in a Florida reef. This was based on the premise that the reef exhibits a homogeneous composition where *O. faveolata* represents 80% of the massive corals, so that the linear erosion rate they estimated was broadly representative at the reef scale. However, many reefs have very heterogeneous compositions, particularly as they have been degraded and community composition shifted (González-Barrios et al. 2020; Cramer et al. 2021). In such systems multiple species response data thus becomes an imperative. Knowing the erosion patterns of the reef framework at the species level would also help to tackles some uncertainties described for methodologies like *ReefBudget*, including the mobile character of major eroders such as parrotfish, which means that their eroding function is spatially variable within their home range (this is not the case for sessile calcifying organisms). In addition, because many parrotfish feed in groups, high variability in abundance surveys can occur, potentially biasing inferred estimations of erosion (Lange et al. 2020). There is in addition the fact that census-based estimations of bioerosion depend on published species-specific bioerosion rates that exist for a subset of species and locations (Lange et al. 2020).

In general, our approach was able to accurately quantify even small vertical changes over time, and the comparison with 3D models of *O. faveolata* and *P. strigosa* confirm that the point measurements are representative of erosion across the entire top surface of recently dead coral colonies (Fig. 3; Supporting Information Fig. S3). These patterns also seem to confirm that parrotfish are the primary eroding agents (Bruggemann et al. 1994*a*). In contrast to the upper substrate surfaces, the vertical sides and lower parts of the dead colony 3D models showed no net erosion or even accretion. We believe this is not a result of actual carbonate accretion but caused by the development of dense turf algal mats in regions that are not extensively grazed. The photogrammetry approach could be extended and developed further to help inform us about varying rates of erosion across colonies in different environments, evaluate change in benthic cover, correlation of erosion rates with colony surface slope and cover (indicating accessibility to bioeroders), loss of surface rugosity over time, and the identification and quantification of feeding scars. A challenge of this approach is however the fact that dense turf algae appear as accretion zones in the models, limiting this method to extensively grazed reef areas and suggesting a minimum survey period of 1 or 2 yr to allow for measurable differences in surface elevation.

Heterogeneous environments require further in situ measurements of erosion rates for a range of species, since these rates likely differ as depth, light, relief, and other factors may change, and influence both assemblages of producing and eroding organisms (Lange et al. 2020). For instance, corals tend to present denser and more resistant skeletons in deeper areas (Baker and Weber 1975), but also parrotfish bioerosion may decline with depth where the light and algae production decline (Nemeth and Appeldoorn 2009). Likewise, covering longer periods of exposure that permit us to have a glimpse of the long-term progression of dead carbonate structures is crucial, as we still have a lot to learn about how erosion varies in space and time.

Undoubtedly, bioerosion is a key process in coral reefs, that directly influences the net accretion and relief of the reef framework, as well as the production, reworking, and relocation of carbonate sediments (Glynn and Manzello 2015). The existence and persistence of contemporary coral reefs is conditioned to high rates of gross carbonate production offsetting the amount of carbonate being eroded. Yet, as coral reef structure and functionality worldwide are increasingly impaired by different local and global stressors, the role of erosion in shaping the reef framework gains importance (Perry et al. 2014; Kuffner and Toth 2016), particularly in the context of mass mortality like the one caused by the SCTLD outbreak. At large spatial scales, the loss of surface elevation in dead colonies could lead to decreases in the surface roughness, and the flattening of the reef framework (Alvarez-Filip et al. 2009; Perry and Alvarez-Filip 2018), which in turn, could increase the water depth over shallow reefs (Storlazzi et al. 2011; Yates et al. 2017) and further exacerbate the already impaired capacity of highly perturbed coral reefs to track future sea-level rise (Perry et al. 2018). This may lead to further impacts on coral reefs (e.g., changes in hydrodynamics, sediment transport, and submergence) and adjacent coastal zones (e.g., flooding, erosion, shoreline change).

Coral recruitment and re-growth of remaining living corals is essential to cover the bare carbonate structure and reduce their vulnerability to bioerosion, and to strengthen net coral reef growth capacity. An easing of bioerosion pressure could undoubtedly aid in these goals (Molina-Hernández et al. 2020), for instance by controlling the abundance of eroding sponges which thrive on increasing eutrophication, and that most like will colonize substrates in the coming years (Tribollet and Golubic 2011). The manipulation of some groups of bioeroder populations could however bring unexpected feedbacks, as the different eroding organisms perform other simultaneous functions in the ecosystem while feeding or boring. In any case, it is key to facilitate an increase in gross carbonate production rates on reefs to improve the capacity of coral reef communities to recover and gain a resilience to further expected perturbations. This may occur through natural processes if local threats can be minimized or may need to be supported through assisted repopulation of impaired coralline communities (Suchley and Alvarez-Filip 2018; Williams and Graham 2019).

Data availability statement

Data are available in the Supporting Information.

References

Adam, T. C., M. Kelley, B. I. Ruttenberg, and D. E. Burkepile. 2015. Resource partitioning along multiple niche axes drives functional diversity in parrotfishes on Caribbean coral reefs. Oecologia **179**: 1173–1185. doi:10.1007/s00442-015-3406-3

Adam, T., A. Duran, C. Fuchs, M. Roycroft, M. Rojas, B. Ruttenberg, and D. Burkepile. 2018. Comparative analysis of foraging behavior and bite mechanics reveals complex functional diversity among Caribbean parrotfishes. Mar. Ecol. Prog. Ser. **597**: 207–220. doi:10.3354/meps12600

Alvarez-Filip, L., N. K. Dulvy, J. A. Gill, I. M. Côté, and A. R. Watkinson. 2009. Flattening of Caribbean coral reefs: Region-wide declines in architectural complexity. Proc. Biol. Sci. **276**: 3019–3025. doi:10.1098/rspb.2009.0339

Alvarez-Filip, L., F. J. González-Barrios, E. Pérez-Cervantes, A. Molina-Hernández, and N. Estrada-Saldívar. 2022. Stony coral tissue loss disease decimated Caribbean coral populations and reshaped reef functionality. Commun. Biol. **5**: 440. doi:10.1038/s42003-022-03398-6

Aronson, R. B., and W. F. Precht. 2001. White-band disease and the changing face of Caribbean coral reefs. Hydrobiologia **460**: 25–38. doi:10.1023/A:1013103928980

Aronson, R. B., I. G. Macintyre, W. F. Precht, T. J. T. Murdoch, and C. M. Wapnick. 2002. The expanding scale of species turnover events on coral reefs in Belize. Ecol. Monogr. **72**: 233–249.

Baker, P. A., and J. N. Weber. 1975. Coral growth rate: Variation with depth. Earth Planet. Sci. Lett. **27**: 57–61. doi:10.1016/0012-821X(75)90160-0

Barott, K. L., and F. L. Rohwer. 2012. Unseen players shape benthic competition on coral reefs. Trends Microbiol. **20**: 621–628. doi:10.1016/j.tim.2012.08.004

Bellwood, D. R., and J. H. Choat. 1990. A functional analysis of grazing in parrotfishes (family Scaridae): The ecological implications, p. 189–214. *In* M. N. Bruton [ed.], Alternative life-history styles of fishes. Springer.

Brainard, R. E., C. Birkeland, C. M. Eakin, P. McElhany, M. W. Miller, M. E. Patterson, and G. A. Piniak. 2011. Status review repo rt of 82 candidate coral species petitioned under the U.S. Endangered Species Act. U.S. Dep. Commer., NOAA Tech. Memo., NOAA-TM-NMFS-PIFSC-27, 530 p.

Bruggemann, J. H., M. W. M. Kuyper, and A. M. Breeman. 1994*a*. Comparative analysis of foraging and habitat use by the sympatric Caribbean parrotfish *Scarus vetuta* and *Sparisoma viride* (Scaridae). Mar. Ecol. Prog. Ser. **112**: 51–66. doi:10.3354/meps112051

Bruggemann, J., M. van Oppen, and A. Breeman. 1994*b*. Foraging by the stoplight parrotfish *Sparisoma viride*. I. Food selection in different, socially determined habitats. Mar. Ecol. Prog. Ser. **106**: 41–55. doi:10.3354/meps106041

Bruggemann, J., A. van Kessel, J. van Rooij, and A. Breeman. 1996. Bioerosion and sediment ingestion by the Caribbean parrotfish *Scarus vetula* and *Sparisoma viride*: Implications of fish size, feeding mode and habitat use. Mar. Ecol. Prog. Ser. **134**: 59–71. doi:10.3354/meps134059

Caballero-Aragón, H., and others. 2020. Puerto morelos coral reefs, their current state and classification by a scoring system. Diversity. **12**: 272. doi:10.3390/d12070272

Carricart-Ganivet, J. P., and D. J. Barnes. 2007. Densitometry from digitized images of X-radiographs: Methodology for measurement of coral skeletal density. J. Exp. Mar. Biol. Ecol. **344**: 67–72. doi:10.1016/j.jembe.2006.12.018

Chamberlain, J. A. 1978. Mechanical properties of coral skeleton: Compressive strength and its adaptive significance. Paleobiology **4**: 419–435. doi:10.1017/S0094837300006163

Chazottes, V., T. Le Campion-alsumard, and M. Peyrot-Clausade. 1995. Bioerosion rates on coral reefs: Interactions between oborers, microborers and grazers (Moorea, French Polynesia). Palaeogeogr. Palaeoclimatol. Palaeoecol. **113**: 189–198.

Chisholm, J. R. M. 2003. Primary productivity of reef-building crustose coralline algae. Limnol. Oceanogr. **48**: 1376–1387.

Conand, C., P. Chabanet, P. Cuet, and Y. Letourneur. 1997. The carbonate budget of a fringing reef in La Reunion Island (Indian Ocean): Sea urchin and fish bioerosion and net calcification. Proc. 8th Int. Coral Reef Symp. **1**: 953–958.

Cosain-Díaz, J. A., J. de Jesús Adolfo Tortolero-Langarica, A. P. Rodríguez-Troncoso, E. Bautista-Guerrero, D. M. Antuna-Roman, P. Salazar-Silva, and A. L. Cupul-Magaña. 2021. Bioerosión interna en corales masivos asociados a las comunidades arrecifales del Pacífico nororiental tropical: Efecto de factores intrínsecos y extrínsecos. Ciencias Mar. **47**: 33–47. doi:10.7773/cm.v47i1.3047

Cramer, K. L., M. K. Donovan, J. B. C. Jackson, B. J. Greenstein, C. A. Korpanty, G. M. Cook, and J. M. Pandolfi. 2021. The transformation of Caribbean coral communities since humans. Ecol. Evol. **11**: 10098–10118. doi:10.1002/ece3.7808

Cruz-Ortega, I., R. A. Cabral-Tena, E. Carpizo-Ituarte, V. Grosso-Becerra, and J. P. Carricart-Ganivet. 2020. Sensitivity of calcification to thermal history differs between sexes in the gonochoric reef-building corals *Dichocoenia stokesi* and *Dendrogyra cylindrus*. Mar. Biol. **167**: 101. doi:10.1007/s00227-020-03713-x

De Bakker, D. M., A. E. Webb, L. A. van den Bogaart, S. M. A. C. Van Heuven, E. H. Meesters, and F. C. van Duyl. 2018. Quantification of chemical and mechanical bioerosion rates of six Caribbean excavating sponge species found on the coral reefs of Curaçao. PLoS One **13**: 1–22. doi:10.1371/journal.pone.0197824

Diaz-Pulido, G., and L. McCook. 2002. The fate of bleached corals: Patterns and dynamics of algal recruitment. Mar. Ecol. Prog. Ser. **232**: 115–128. doi:10.3354/meps232115

Eakin, C. M. 2001. A tale of two enso events: Carbonate budgets and the influence of two warming disturbances and intervening variability, Uva Island. Panama. Bull. Mar. Sci. **69**: 171–186.

Enochs, I. C., D. P. Manzello, R. D. Carlton, D. M. Graham, R. Ruzicka, and M. A. Colella. 2015. Ocean acidification enhances the bioerosion of a common coral reef sponge: Implications for the persistence of the Florida Reef Tract. Bull. Mar. Sci. **91**: 271–290. doi:10.5343/bms.2014.1045

Estrada-Saldívar, N., A. Molina-Hernández, E. Pérez-Cervantes, F. Medellín-Maldonado, F. J. González-Barrios, and L. Alvarez-Filip. 2020. Reef-scale impacts of the stony coral tissue loss disease outbreak. Coral Reefs **39**: 861–866. doi:10.1007/s00338-020-01949-z

Estrada-Saldívar, N., B. A. Quiroga-García, E. Pérez-Cervantes, O. O. Rivera-Garibay, and L. Alvarez-Filip. 2021. Effects of the stony coral tissue loss disease outbreak on coral communities and the benthic composition of cozumel reefs. Front. Mar. Sci. **8**: 632777. doi:10.3389/fmars.2021.632777

Glynn, P. W., and D. P. Manzello. 2015. Bioerosion and coral reef growth: A dynamic balance, p. 67–97. *In* C. Birkeland [ed.], Coral reefs in the Anthropocene. Springer.

González-Barrios, F. J., and L. Álvarez-Filip. 2018. A framework for measuring coral species-specific contribution to reef functioning in the Caribbean. Ecol. Indic. **95**: 877–886. doi:10.1016/j.ecolind.2018.08.038

González-Barrios, F. J., R. A. Cabral-Tena, and L. Alvarez-Filip. 2020. Recovery disparity between coral cover and the physical functionality of reefs with impaired coral assemblages. Glob. Chang. Biol. **27**: 640–651. doi:10.1111/gcb.15431

Grange, J. S., H. Rybarczyk, and A. Tribollet. 2015. The three steps of the carbonate biogenic dissolution process by microborers in coral reefs (New Caledonia). Environ. Sci. Pollut. Res. **22**: 13625–13637. doi:10.1007/s11356-014-4069-z

Hernández-Ballesteros, L. M., E. M. Elizalde-Rendón, J. L. Carballo, and J. P. Carricart-Ganivet. 2013. Sponge bioerosion on reef-building corals: Dependent on the environment or on skeletal density? J. Exp. Mar. Biol. Ecol. **441**: 23–27. doi:10.1016/j.jembe.2013.01.016

Hubbard, D. K., and W.-C. Dullo. 2016. The changing face of reef building, p. 127–153. *In* D. K. Hubbard, C. S. Rogers, J. H. Lipps, and G. D. Stanley Jr. [eds.], Coral reefs at the crossroads. Springer.

Hudson, J. H. 1977. Long-term bioerosion rates on a Florida reef: A new method, p. 491–498. *In* Proceedings of Third International Coral Reef Symposium. Rosenstiel School of Marine and Atmospheric Science.

Hughes, T. P. 1987. Skeletal density and growth form of corals. Mar. Ecol. Prog. Ser. **35**: 259–266.

Hutchings, P. A. 1986. Biological destruction of coral reefs. Coral Reefs **4**: 239–252. doi:10.1007/BF00298083

Hutchings, P., M. Peyrot-Clausade, and A. Osnorno. 2005. Influence of land runoff on rates and agents of bioerosion of coral substrates. Mar. Pollut. Bull. **51**: 438–447. doi:10.1016/j.marpolbul.2004.10.044

James, M., S. Robson, and M. Smith. 2017. 3-D uncertainty-based topographic change detection with structure-from-motion photogrammetry: Precision maps for ground control and directly georeferenced surveys. Earth Surf. Process. Landforms **42**: 1769–1988.

Kiene, W. E., and P. A. Hutchings. 1994. Bioerosion experiments at lizard Island, great barrier reef. Coral Reefs **13**: 91–98. doi:10.1007/BF00300767

Kuffner, I. B., and L. T. Toth. 2016. A geological perspective on the degradation and conservation of western Atlantic coral reefs. Conserv. Biol. **30**: 706–715. doi:10.1111/cobi.12725

Kuffner, I. B., L. T. Toth, J. H. Hudson, W. B. Goodwin, A. Stathakopoulos, L. A. Bartlett, and E. M. Whitcher. 2019. Improving estimates of coral reef construction and erosion with in situ measurements. Limnol. Oceanogr. **64**: 2283–2294. doi:10.1002/lno.11184

Lague, D., N. Brodu, and J. Leroux. 2013. Accurate 3D comparison of complex topography with terrestrial laser scanner: Application to the Rangitikei canyon (N-Z). ISPRS J. Photogram. Remote Sens. **82**: 10–26. doi:10.1016/j.isprsjprs.2013.04.009

Lange, I. D., and C. T. Perry. 2020. A quick, easy and non-invasive method to quantify coral growth rates using photogrammetry and 3D model comparisons. Methods Ecol. Evol. **11**: 714–726. doi:10.1111/2041-210X.13388

Lange, I. D., C. T. Perry, and L. Alvarez-Filip. 2020. Carbonate budgets as indicators of functional reef "health": A critical review of data underpinning census-based methods and current knowledge gaps. Ecol. Indic. **110**: 105857. doi:10.1016/j.ecolind.2019.105857

Lessios, H. A. 2016. The great *Diadema antillarum* die-off: 30 years later. Ann. Rev. Mar. Sci. **8**: 267–283. doi:10.1146/annurev-marine-122414-033857

Manzello, D. P., I. C. Enochs, G. Kolodziej, R. Carlton, and L. Valentino. 2018. Resilience in carbonate production despite three coral bleaching events in 5 years on an inshore patch reef in the Florida Keys. Mar. Biol. **165**: 99. doi:10.1007/s00227-018-3354-7

Molina-Hernández, A., F. J. González-Barrios, C. T. Perry, and L. Álvarez-Filip. 2020. Two decades of carbonate budget change on shifted coral reef assemblages: Are these reefs being locked into low net budget states? Proc. R. Soc. B Biol. Sci. **287**: 20202305. doi:10.1098/rspb.2020.2305

Morillo-Velarde, P. S., P. Briones-Fourzán, L. Álvarez-Filip, S. Aguíñiga-García, A. Sánchez-González, and E. Lozano-Álvarez. 2018. Habitat degradation alters trophic pathways but not food chain length on shallow Caribbean coral reefs. Sci. Rep. **8**: 4109. doi:10.1038/s41598-018-22463-x

Mulcahy, N. P. M. 2014. The geomorphic significance of hurricanes on coral-fringed calcium carbonate coastlines: Hurricane Wilma 15–25 October 2005, northeastern Yucatan peninsula. Victoria Univ. of Wellington.

Nemeth, M., and R. Appeldoorn. 2009. The distribution of herbivorous coral reef fishes within fore-reef habitats: The role of depth, light and Rugosity. Caribb. J. Sci. **45**: 247–253. doi:10.18475/cjos.v45i2.a11

Nicholson, G. M., and K. D. Clements. 2020. Resolving resource partitioning in parrotfishes (Scarini) using microhistology of feeding substrata. Coral Reefs **39**: 1313–1327. doi:10.1007/s00338-020-01964-0

Pernice, M., J. R. Nils, C. R. Voolstra, A. Cárdenas, and C. Pogoreutz. 2020. Down to the bone: The role of overlooked endolithic microbiomes in reef coral health. ISME J. **325–334**: 325–334. doi:10.1038/s41396-019-0548-z

Perry, C. T., E. N. Edinger, P. S. Kench, G. N. Murphy, S. G. Smithers, R. S. Steneck, and P. J. Mumby. 2012. Estimating rates of biologically driven coral reef framework production and erosion: A new census-based carbonate budget methodology and applications to the reefs of Bonaire. Coral Reefs **31**: 853–868. doi:10.1007/s00338-012-0901-4

Perry, C. T., G. N. Murphy, P. S. Kench, S. G. Smithers, E. N. Edinger, R. S. Steneck, and P. J. Mumby. 2013. Caribbean-wide decline in carbonate production threatens coral reef growth. Nat. Commun. **4**: 1402. doi:10.1038/ncomms2409

Perry, C. T., G. N. Murphy, P. S. Kench, E. N. Edinger, S. G. Smithers, R. S. Steneck, and P. J. Mumby. 2014. Changing dynamics of Caribbean reef carbonate budgets: Emergence of reef bioeroders as critical controls on present and future reef growth potential. Proc. R. Soc. B Biol. Sci. **281**: 20142018. doi:10.1098/rspb.2014.2018

Perry, C. T., R. S. Steneck, G. N. Murphy, P. S. Kench, E. N. Edinger, S. G. Smithers, and P. J. Mumby. 2015. Regional-scale dominance of non-framework building corals on Caribbean reefs affects carbonate production and future reef growth. Glob. Chang. Biol. **21**: 1153–1164. doi:10.1111/gcb.12792

Perry, C. T., and L. Alvarez-Filip. 2018. Changing geo-ecological functions of coral reefs in the Anthropocene. Funct. Ecol. **33**: 1365–2435.13247. doi:10.1111/1365-2435.13247

Perry, C. T., and others. 2018. Loss of coral reef growth capacity to track future increases in sea level. Nature **558**: 396–400. doi:10.1038/s41586-018-0194-z

Perry, C. T., and I. D. Lange. 2019. ReefBudget Caribbean v2: Online resource and methodology. http://geography.exeter.ac.uk/reefbudget/

Phillips, J. D., Ł. Pawlik, and P. Šamonil. 2019. Weathering fronts. Earth Sci. Rev **198**: 102925. doi:10.1016/j.earscirev.2019.102925

Rodríguez-Martínez, R. E., A. T. Banaszak, M. D. McField, A. U. Beltrán-Torres, and L. Álvarez-Filip. 2014. Assessment of *Acropora palmata* in the Mesoamerican reef system. PLoS One **9**: e96140. doi:10.1371/journal.pone.0096140

Roff, G., J. Zhao, and P. J. Mumby. 2015. Decadal-scale rates of reef erosion following El Niño-related mass coral mortality. Glob. Chang. Biol. **21**: 4415–4424. doi:10.1111/gcb.13006

Roff, G., J. Joseph, and P. J. Mumby. 2019. Multi-decadal changes in structural complexity following mass coral mortality on a Caribbean reef. Biosciences **1**: 1–16.

Rogers, C. S., T. H. Suchanek, and F. A. Pecora. 1982. Effects of Hurricanes David and Frederic (1979) on shallow Acropora palmata reef communities: St. Croix, U.S. Virgin Islands. Bull. Mar. Sci. **32**: 532–548. doi:10.1016/0198-0254(82)90307-7

Russ, G. R., S.-L. A. Questel, J. R. Rizzari, and A. C. Alcala. 2015. The parrotfish–coral relationship: Refuting the ubiquity of a prevailing paradigm. Mar. Biol. **162**: 2029–2045. doi:10.1007/s00227-015-2728-3

Sano, M., M. Shimizu, and Y. Nose. 1987. Long-term effects of destruction of hermatypic corals by *Acanthaster planci* infestation on reef fish communities at Iriomote Island, Japan. Mar. Ecol. Prog. Ser. **37**: 191–199. doi:10.3354/meps037191

Schielzeth, H., and W. Forstmeier. 2009. Conclusions beyond support: Overconfident estimates in mixed models. Behav. Ecol. **20**: 416–420. doi:10.1093/beheco/arn145

Schönberg, C. H. L., J. K. H. Fang, M. Carreiro-Silva, A. Tribollet, and M. Wisshak. 2017. Bioerosion: The other ocean acidification problem. ICES J. Mar. Sci. **74**: 895–925. doi:10.1093/icesjms/fsw254

Sheppard, C. R. C., M. Spalding, C. Bradshaw, and S. Wilson. 2002. Erosion vs. recovery of coral reefs after 1998 El Niño: Chagos Reefs, Indian Ocean. AMBIO J. Hum. Environ. **31**: 40–48. doi:10.1579/0044-7447-31.1.40

Storlazzi, C. D., E. Elias, M. E. Field, and M. K. Presto. 2011. Numerical modeling of the impact of sea-level rise on fringing coral reef hydrodynamics and sediment transport. Coral Reefs **30**: 83–96. doi:10.1007/s00338-011-0723-9

Suchley, A., and L. Alvarez-Filip. 2018. Local human activities limit marine protection efficacy on Caribbean coral reefs. Conserv. Lett. **11**: e12571. doi:10.1111/conl.12571

Taylor, B. M., C. E. Benkwitt, H. Choat, K. D. Clements, N. A. J. Graham, and M. G. Meekan. 2020. Synchronous biological feedbacks in parrotfishes associated with pantropical coral bleaching. Glob. Chang. Biol. **26**: 1285–1294. doi:10.1111/gcb.14909

Tebbett, S. B., C. H. R. Goatley, R. P. Streit, and D. R. Bellwood. 2020. Algal turf sediments limit the spatial extent of function delivery on coral reefs. Sci. Total Environ. **734**: 139422. doi:10.1016/j.scitotenv.2020.139422

Toth, L. T., I. B. Kuffner, A. Stathakopoulos, and E. A. Shinn. 2018. A 3,000-year lag between the geological and ecological shutdown of Florida's coral reefs. Glob. Chang. Biol. **24**: 5471–5483. doi:10.1111/gcb.14389

Toth, L. T., A. Stathakopoulos, I. B. Kuffner, R. R. Ruzicka, M. A. Colella, and E. A. Shinn. 2019. The unprecedented loss of Florida's reef-building corals and the emergence of a novel coral-reef assemblage. Ecology **100**: e02781. doi:10.1002/ecy.2781

Trenhaile, A. S. 2011. Cliffs and rock coasts, p. 171–191. *In* Treatise on estuarine and coastal science. Elsevier.

Tribollet, A. 2008. The boring microflora in modern coral reef ecosystems: A review of its roles, p. 67–94. *In* Current developments in bioerosion. Springer.

Tribollet, A., and S. Golubic. 2011. Reef bioerosion agents and processes. Springer: Netherlands.

Viles, H. A., and S. T. Trudgill. 1984. Long term remeasurements of micro-erosion meter rates, Aldabra Atoll, Indian Ocean. Earth Surf. Process. Landforms **9**: 89–94.

Ward, W. C., and M. J. Brady. 1979. Strandline sedimentation of carbonate grainstones, Upper Pleistocene, Yucatan Peninsula, Mexico. Am. Assoc. Pet. Geol. Bull. **63**: 362–369. doi:10.1306/C1EA5616-16C9-11D7-8645000102C1865D

Williams, G. J., and N. A. J. Graham. 2019. Rethinking coral reef functional futures. Funct. Ecol. **33**: 942–947. doi:10.1111/1365-2435.13374

Woodhead, A. J., C. C. Hicks, A. V. Norström, G. J. Williams, and N. A. J. Graham. 2019. Coral reef ecosystem services in the Anthropocene. Funct. Ecol. **33**: 1023–1034. doi:10.1111/1365-2435.13331

Yates, K. K., D. G. Zawada, N. A. Smiley, and G. Tiling-Range. 2017. Divergence of seafloor elevation and sea level rise in coral reef ecosystems. Biogeosciences **14**: 1739–1772. doi:10.5194/bg-14-1739-2017

Acknowledgments

The authors thank Esmeralda Perez-Cervantes, Nuria Estrada-Saldivar, and Israel Cruz-Ortega for their help in collecting, and systemizing the data used in this study, and Juan Pablo Carricart-Ganivet whose comments and suggestions greatly improved the manuscript.

Conflict of Interest

None declared.

Submitted 05 May 2022
Revised 26 August 2022
Accepted 05 September 2022

Associate editor: David Michael Baker